J|A|C|S
COMMUNICATIONS

Published on Web 04/06/2002

Binding Modes for the First Coupled Electron and Proton Addition to FeMoco of Nitrogenase

Timothy Lovell,*,† Jian Li,‡ David A. Case,*,† and Louis Noodleman*,†

The Scripps Research Institute, La Jolla California 92037, and Texas Biotechnology Corporation, Houston Texas 77030

Received October 9, 2001

Nitrogenase, the metalloprotein system responsible for biological nitrogen fixation,[1] catalyzes the reduction of dinitrogen (N_2) to ammonia (NH_3) under ambient conditions. The most extensively studied MoFe form consists of two components, the Fe protein and the MoFe protein. The larger, catalytic, $\alpha_2\beta_2$ MoFe protein comprises two unique metal-containing clusters (the 8Fe P cluster and the 7FeMo9S cofactor) within each $\alpha\beta$ pair. FeMoco is the proposed site of binding and reduction of N_2 and other molecules.

A general mechanism of N_2 fixation outlining the various protonation and oxidation states of the MoFe protein has been postulated from kinetic data for *Klebsiella pneumoniae* nitrogenase.[2] Successive one-electron reductions at resting FeMoco (E_0) produce states that are $1e^-$, $2e^-$, $3e^-$, and $4e^-$ reduced (E_1, E_2, E_3, and E_4, respectively). Coupled proton transfers give rise to states E_1H_1, E_2H_2, and E_3H_3 and E_4H_4. Beyond E_3H_3 or E_4H_4, kinetic data support N_2 binding to FeMoco concomitant with H_2 release. Activation of N_2 and dissociation of 2 NH_3 results, and the cycle proceeds via various intermediates back to E_0.

Although the X-ray structure of FeMoco is available for E_0,[3] the structures of the intermediate states remain unknown. Crystallography[4] and EXAFS[5] experiments have observed only minor structural changes in FeMoco. Theoretical methods, such as density functional theory (DFT),[6,7] in combination with broken-symmetry (BS)[8] wavefunctions can offer insights into the structures of potential catalytic intermediates. Computational studies thus far[9] have mainly focused on the apparently unsaturated iron sites and the μS^2 atoms as the initial location for substrate(s) binding, migration, and transformation events. Several reasons support this bias. Structurally analogous forms of alternate nitrogenase cofactors contain iron and sulfur. The trigonal Fe sites appear underligated and may be reactive. Protein residues surrounding this portion of FeMoco are scarce. The Mo atom that is surrounded by an octahedral ligand array appears coordinatively saturated. However, Mo can expand its valence to as much as eight-coordinate,[10] so that six-fold coordination need not rule it out.[10]

The immediate questions of chemical relevance are: when FeMoco acquires the first reducing equivalent, what is the preferred orientation of the electron spin? What are the most favorable binding sites for protons and how are the energies of these possible redox states modulated by the protein environment? Consistent with Mössbauer data,[11] a recent study of the electronic structure of FeMoco suggested the spin-up lowest unoccupied molecular orbital (LUMO) comprises Mo and O as majority atomic components and a smaller Fe contribution; the spin-down counterpart displays large trigonal Fe contributions.[12] Starting from $[Mo^{4+}6Fe^{2+}Fe^{3+}9S^{2-}]^+$ for E_0, electrons may therefore be added either spin up ($\uparrow$) or spin down ($\downarrow$), giving E_1H_1 clusters of total spin $S = 2$ or $S = 1$, respectively. In accord with the Thorneley−Lowe scheme, the results of BS-DFT calculations on possible reduced and protonated E_1H_1 states of FeMoco in the protein environment are now reported. Inherent in the calculations is the assumption that the spin-coupling scheme deduced for E_0 (Figure 1) persists on reduction. Geometry optimization determined the proton location in each case. Of the many proton positions investigated, only those with lowest energy are reported in Table 1. Energies[13] are given relative to the most stable state in the protein environment.

The Case for Fe and the μS^2 Atoms. The lowest-energy structure for state E_1H_1 comprises a $[Mo^{4+}5Fe^{2+}2Fe^{3+}9S^{2-}H^-]^+$ core having total spin $S = 2$ with a proton residing in a novel position: closest to Fe_4 but asymmetrically displaced between the six trigonal Fe sites (Figure 2). This state is denoted $E_1H_{1-c}(\uparrow)$ having energy, 0.0 kcal/mol. The arrow indicates the electron is added to the spin-up LUMO; subscript (c) signifies the proton location is approximately in the center of the 6Fe cavity. The $S = 1$ $E_1H_{1-c}(\downarrow)$ spin-down alternative lies only +1.0 kcal/mol higher. A large negative electrostatic potential (ESP) within the central prismane provides the driving force for this proton location. Significant spin density on the bound H atom ($s = -0.05$) and a short distance of $Fe_4-H = 1.82$ Å indicates an Fe-hydride interaction is present. The position of this first proton differs markedly from other computational studies which predicted the μS^2 atoms were the most favorable, initial protonation sites. The formation of Fe-hydride-type species may be a first step toward general H_2 evolution at FeMoco and is similar to the metal-hydride intermediates observed in heterogeneous H_2 evolution at metal surfaces.[9j] Consistent with this notion, the ferrous (Fe^{2+})-to-ferric-hydride $(Fe^{3+}-H^-)^{2+}$ conversion is thus achieved independently of any change in total cluster charge. Oxidation of one or more Fe sites by an hydridic proton likely enables the addition of subsequent reducing equivalents to FeMoco and facilitates production of states more reduced than E_1H_1. In an absolute sense, the catalytic reduced state (M^R) observed during enzyme turnover to give an $S \geq 1$ EPR signal is consistent both with the protein environment selecting state $E_1H_{1-c}(\uparrow)$ ($S = 2$) over the alternative radiolytically reduced state (M^I) $E_1H_{1-c}(\downarrow)$ ($S = 1$) and our relative energetics (Table 1). Of the remaining trigonal Fe sites, an alternative proton position bound (as hydride) closest to Fe_8 and lying in the $Fe_3Fe_4Fe_7Fe_8$ face (f) ($E_1H_{1-f}(\uparrow)$, +8.2 kcal/mol) is also favorable. Proton binding external (ext) to the cluster at Fe_5 ($E_1H_{1-ext}(\uparrow)$, +15.5 kcal/mol) lies higher in energy. Overall, interatomic distances appear slightly changed by reduction and subsequent protonation at the Fe sites.

The inorganic S atoms fall into two distinct categories, μS^2 bridging (b) and μS^3 terminal-capping (t). The high electronegativity and formal negative charge of the S^{2-} atoms indicate favorable electrostatics for proton binding. The lowest-energy μS^2 structure, $E_1H_{1-b3}(\uparrow)$, protonated at S_{14}, lies +9.9 kcal/mol higher in energy

* To whom correspondence should be addressed. E-mail: case@scripps.edu.
† The Scripps Research Institute.
‡ Texas Biotechnology Corporation.

10.1021/ja012311v CCC: $22.00

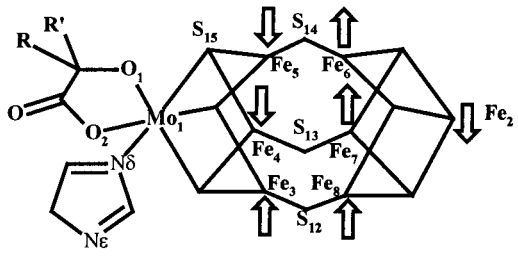

Figure 1. Spin coupling alignment used to describe resting E_0 and possible reduced and protonated E_1H_1 states of FeMoco.

Table 1. Breakdown of the Final Energy in the Protein ΔE(total) (kcal/mol) into Gas Phase, Protein, and Zero-Point Energy Component Parts for Various Spin-Up ($S = 2$) and Spin-Down ($S = 1$) Protonated E_1H_1 States of FeMoco

	FeMoco	ΔE (gas phase)		ΔE (protein)		ΔE (zpe)	ΔE (total)	
site	state	↑ ($S = 2$)	↓ ($S = 1$)	↑ ($S = 2$)	↓ ($S = 1$)		↑ ($S = 2$)	↓ ($S = 1$)
Fe4	E1H1-c	0.0	−0.8	0.0	+1.8	0.0	0.0	+1.0
Fe8	E1H1-f	+7.0	+5.6	+1.2	+6.6	0.0	+8.2	+12.2
Fe5	E1H1-ext	+16.4	+19.0	−0.9	+2.2	0.0	+15.5	+21.2
S12	E1H1-b1	+8.1	+11.9	+4.2	+3.0	3.2	+15.5	+18.1
S13	E1H1-b2	+6.9	+7.7	+0.3	+3.0	3.2	+10.4	+13.9
S14	E1H1-b3	+7.8	+6.8	−1.1	+2.4	3.2	+9.9	+12.4
S15	E1H1-t	+33.0	+32.7	+0.1	+2.9	3.2	+36.3	+38.8
Nδ	E1H1−Nδ	+41.2	+41.5	−9.4	+0.9	5.1	+36.9	+47.5
O2	E1H1−O2	+26.1	+26.8	−6.2	−4.7	4.6	+24.5	+26.7
O1	E1H1−O1	+1.5	+6.8	−5.9	−4.9	4.6	+0.2	+6.5

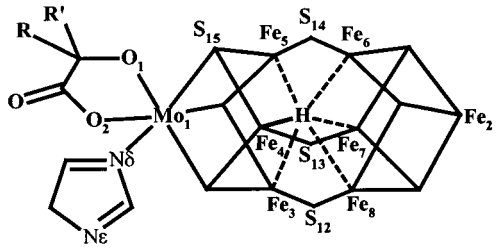

Figure 2. Novel location of a proton for state E_1H_1 of FeMoco.

than $E_1H_{1-c}(\uparrow)$; $E_1H_{1-b2}(\uparrow)$ lies slightly higher at +10.4 kcal/mol, while $E_1H_{1-b1}(\uparrow)$, at +15.5 kcal/mol, is the most unfavorable of the μS^2 atoms. Protonation of the μS^3 atoms, at S_{15} for example, results in structures that are significantly destabilized energetically. Proton binding to the μS^3 atoms thus appears less favorable than that for the μS^2 alternative. Compared to E_0, Fe−S bonds lengthen by about 0.1 Å generally on protonation of S atoms. In vacuo, all μS^2 atoms appear equally attractive to an incoming proton. In *Azotobacter vinelandii* (*Av*) protein, S_{14} is within hydrogen-bonding distance of the imidazole ring of His195; S_{13} lies close to the side chain of Arg96 and a single water molecule (HOH617); S_{12} is near to the backbone protons of Arg359, Leu358, Gly357, and Gly356. From the calculations, the role of the protein matrix is to distinguish the μS^2 sites by imposing a specific order for protonation ($S_{14} > S_{13} > S_{12}$).[9i] If the first proton accesses FeMoco through the μS^2 atoms via these residues and their associated hydrogen-bonding pathways, then His195 may well be on the preferred pathway. Once bound to FeMoco at S_{14}, in the absence of substantial energy barriers, the energetics suggest proton relocation should be both a facile and favorable process.

The Case for Mo and the Homocitrate. Without imposing geometric constraints, we have been unable to bind a proton to Mo successfully at this redox level so that a role for Mo-hydride chemistry in catalysis is not evident. After initially being bound to Mo formally as a hydride, the final position of the proton is governed by the starting orientation of the Mo−H bond. In accord with the pool of water molecules that surround the homocitrate in *Av*, several possibilities have been calculated. Proton relocation to the alkoxyl (O_1) or carboxylate (O_2) oxygens covalently linked to Mo results in a five-coordinate Mo atom. In $E_1H_{1-O1}(\uparrow)$, the increase in the Mo−O_1 bond length (from 2.00 to 2.13 Å) is accompanied by a similar elongation in Mo−O_2 (from 2.16 to 2.34 Å). A proton bound to O_1 therefore activates the Mo−O_2 bond and produces a low-lying state ($E_1H_{1-O1}(\uparrow)$, +0.2 kcal/mol). Direct protonation of O_2 in E_1H_{1-O2} severs the Mo−O_2 bond (2.49 Å), but this structure lies very high in energy (∼+25 kcal/mol). In contrast to the observed phenomena noted for model complexes,[10] the calculations do not support *both* Mo-hydride-type interactions and the dissociation of the carboxylate-type species; only *after* proton migration does carboxylate dissociation from Mo occur. Protonation at His442·Nδ1 results in Mo−Nδ1 bond cleavage (3.33 Å) and also renders the Mo site five-coordinate. The imidazole ring of His442 is prevented from leaving the first coordination sphere via a hydrogen bond to the oxygen atom (O_2) of the homocitrate. $E_1H_{1-N\delta}(\uparrow)$ lies very high in energy (+37 kcal/mol).

Summary. In contrast to protonating the μS^2 atoms, we have found two alternative protonation states for FeMoco. A novel hydridic proton asymmetrically located in the 6Fe prismane is most favored and produces minor structural changes on reduction, consistent with EXAFS. This Fe-hydride-type FeMoco intermediate is somewhat analogous to the Fe-hydrides present in heterogeneous H_2 evolution at Fe surfaces. Protonation at O_1 of the homocitrate weakens and activates Mo−O bonds; a five-coordinate Mo site results, perhaps indicative of a role for Mo at a later stage of the catalytic cycle. Additional studies in the protein environment focused on possible proton relocation mechanisms, which may be of relevance both to general and obligatory H_2 evolution by the nitrogenase active site, are now being pursued.

Acknowledgment. This work was supported by NIH Grant GM 39914. We thank Velin Spassov, Thomas Rod, Brian Hales, and Eckard Münck for discussions. For computer codes, we thank D. McRee (Xtalview), E.J. Baerends (ADF), and D. Bashford (MEAD).

Supporting Information Available: Details of calculations and structures (PDF). This material is available free of charge via the Internet at http://acs.pubs.org.

References

(1) (a) Howard, J. B.; Rees, J. B. *Chem. Rev.* **1996**, *96*, 2965. (b) Burgess, B. K.; Lowe, D. J. *Chem. Rev.* **1996**, *96*, 2983.
(2) 2 Thorneley, R. N. F.; Lowe, D. In *Molybdenum Enzymes*; Spiro, T. G., Ed.; Wiley-Interscience: New York, 1985.
(3) Mayer, S. M.; Lawson, D. M.; Gormal, C. A.; Roe, S. M.; Smith, B. E. *J. Mol. Biol.* **1999**, *292*, 871 and references therein.
(4) Grossman, J. G.; Hasnain, S. S.; Yousafzai, F. K.; Smith, B. E.; Eady, R. R. *J. Mol. Biol.* **1999**, *266*, 642.
(5) Christiansen, J.; Tittsworth, R. J.; Hales, B. J.; Cramer, S. P. *J. Am. Chem. Soc.* **1995**, *117*, 10017.
(6) Ziegler, T. *Chem. Rev.* **1991**, *91*, 651.
(7) Versluis, L.; Ziegler, T *J. Chem. Phys.* **1988**, *88*, 322.
(8) Noodleman, L. *J. Chem. Phys.* **1981**, *74*, 5737.
(9) (a) Deng, H.; Hoffmann, R. *Angew. Chem., Int. Ed. Engl.* **1993**, *32*, 1062. (b) Stavrev, K. K.; Zerner, M. C. *Int. J. Quantum Chem.* **1998**, *70*, 1159. (c) Dance, I. *J. Biol. Inorg. Chem.* **1996**, *1*, 581. (d) Siegbahn, P. E. M.; Westerberg, J.; Svensson, M.; Crabtree, R. H. *J. Phys. Chem. B* **1998**, *102*, 1615. (e) Rod, T. H.; Nørskov, J. K. *J. Am. Chem. Soc.* **2000**, *122*, 12751. (f) Szilagyi, R. K.; Musaev, D. K.; Morokuma, K. *Inorg. Chem.* **2001**, *40*, 766. (g) Durrant, M. C. *Inorg. Chem. Commun.* **2001**, *4*, 60. (h) Barriere, F.; Pickett, C. J.; Talarmin, J. *Polyhedron* **2001**, *20*, 27. (i) Durrant, M. C.; *Biochem. J.* **2001**, *355*, 569. (j) Rod, T. H.; Logadottir, A.; Nørskov, J. K. *J. Chem. Phys.* **2000**, *112*, 5343.
(10) Pickett, C. J. *J. Biol. Inorg. Chem.* **1996**, *1*, 601 and references therein.
(11) Yoo, S. J.; Angove, H. C.; Papaefthymiou, V.; Burgess, B. K.; Münck, E. *J. Am. Chem. Soc.* **2000**, *122*, 4926.
(12) Lovell, T.; Li, J.; Liu, T.; Case, D. A.; Noodleman, L. *J. Am. Chem. Soc.* **2001**, *123*, 12392.
(13) In Table 1, the final energy ΔE (total) of FeMoco in the protein results from the sum of its gas phase, protein, and zero-point energy (of the FeMoco−H bond) contributions.

JA012311V